CENTRAL INSTITUTE OF PHYSICS

INSTITUTE FOR PHYSICS AND TECHNOLOGY OF RADIATION DEVICES*)

Bucharest, P.O.B.5207, ROMANIA

Lasers Department

P.N.Lebedev - Physical Institute, Moscow,U.S.S.R. **)

IFTAR - LOP-8-1979 RO8101583 June

Interferometric investigation of shock waves induced by a TEA-CO_2 laser produced plasma in air in front of a solid target+)

*D.APOSTOL**, *I.APOSTOL**, *E.COJOCARU**, *V.DRAGANESCU**, *I.N.MIHAILESCU**, *I.MORJAN** *and V.I.KONOV***

Abstract : *The shock waves induced in the surrounding atmosphere by an air plasma were investigated by laser interferometry. The air breakdown plasma was produced by a TEA-CO_2 laser in front of a solid target . The results were compared to the predictions of theory of intense explosions in gases and a good agreement was inferred. It was also determined that the symmetry of the expansion of the initial shock wave is determined by the plasma source shape and,accordingly, depends on the laser power density incident on the target surface. However, for further stages all the shock waves expand spherically.*

+) accepted for publication in Journal of Applied Physics (1979).

As it is known, the response of a solid target exposed to the focused radiation of a pulsed CO_2 laser is strongly influenced by the ambient atmosphere. Thus, when a plane target is irradiated by a typical TEA-CO_2 laser pulse of microsecond duration, the induced process does not depend on the target material but rather is determined by the production of a low threshold breakdown in front of the target. The incident laser energy is then absorbed by the air plasma, which becomes the source of a blast wave, whose overpressure renders a mechanical impulse to the target, while a shock wave is propagating through the surrounding gas. Laser-supported detonation waves as well as other laser-supported absorbtion waves have received in recent years a considerable experimental attention and a satisfactory theoretical explanation /1-5/. This communication reports the results of an interferometric investigation of the shock wave induced by the breakdown plasma and subsequently propagating through the neighbouring gas at times following the laser pulse and plasma duration.

The experimental arrangement is schematically depicted in Figure 1. The TEA-CO_2 laser /6/ was of the double discharge Lamberton and Pearson type, with xylene vapours added to the active mixture in the proportions of $CO_2 : N_2 : He = 1 : 1 : 4$. It was able to deliver output pulses of several joules having a typical shape consisting of a first peak with a halfwidth not exceeding 150 ns and a "tail" lasting for several μs. A diaphragm of variable aperture was introduced inside the resonant cavity and placed in the neighbourhood of the output coupling mirror.

The laser beam divergence was found to be 7.2 mrad and the laser cross section was $(25 \times 25) mm^2$. Small fractions of the output beam were directed towards a detector and an energy-meter which enabled the simultaneous recording of both the pulse shape and energy for every pulse. The temporal behaviour obtained with a P5 Molectron pyroelectric detector and displayed on a Tektronix 7504 oscilloscope is also given in Figure 1.

The energy was measured by a TRG thermopile head connected to a TR-6018 Takeda-Riken microvoltmeter. By focusing the laser beam through an AR-coated germanium lens onto the target surface, a power density of $(10^7 \div 10^{10}) W/cm^2$ was achieved and this was enough for ignition of the breakdown in front of the target for a pressure range of 10^{-1} torr to 1 atm of air inside the irradiation chamber. Plasma evolution was followed with the aid of an SFR high speed photographic camera, whose entrance slit was placed either parallelly or normally with respect to the target surface. From the photographic recordings, the time evolution and the expansion symmetry of the luminous front of the plasma were derived.

The plasma production and associated shock wave evolution were arranged to occur in one of the arms of a Michelson interferometer illuminated by a 20 mW/6328 Å He-Ne laser. The laser beam was collimated, so that the interferometric pattern was an uniform field. A complete modulation cycle of this unique fringe corresponded to an optical path change in one of the interferometer arms of $\lambda/2$. A diaphragm and a filter eliminated parasitic reflections and radiation from the plasma. The change in the optical path induced in one of the interferometer arms both by the plasma and by the shock wave was observed as an intensity variation of the beam emerging from the interferometer. This variation was finally detected by a fast BPY 13A photodiode, displayed on the Tektronix 7504 oscilloscope and photographed. In order to record only the shock wave contribution to the interferogram the beam of the He-Ne laser was located at a suitable distance from the limit of the expansion of the plasma. Some typical interferograms are shown in Figure 2. Under the conditions mentioned previously the fringes can be looked upon as direct experimental evidence of the shock wave induced by a laser plasma in the ambient atmosphere.

Thus, a great number of interferograms were recorded, for different incident power densities and pressures of the surrounding gas. These data were analysed by means of a model based on the theory of intense explosion in gases /7/. The spatial coordinate of a gas particle representing its distance to the laser beam axis was denoted by r. The coordinate for each particle equals the shock wave radius $r^*(t)$ at the moment it passes through the particle. The origin was taken to be the time the plasma was initiated. To get the optical path change induced by the shock wave along the He-Ne beam trajectory, $\Delta s(t)$, one has to compute the following integral

$$\Delta s(t) = 4 \int_0^{r^*(t)} \Delta n(r,t)\,dr \qquad (1)$$

where $\Delta n(r,t)$ is the refractive index variation at the time t for a point, r, inside the shock wave. As it is known that

$$\Delta n(r,t) = n(r,t) - n_1 = \beta \frac{\rho_1}{\rho_0} \left| \frac{\rho(r,t)}{\rho_1} - 1 \right| \qquad (2)$$

where n_1, ρ_1; and $n(r,t)$, $\rho(r,t)$ are the refractive index and the gas density prior the shock wave and subsequently at the time t. The quantity ρ_0 is the standard air density and β is a constant equal to 2.92×10^{-4} for air under normal conditions. For $\rho(r,t)$ and $r^*(t)$ the corresponding expressions are taken from Sedov book / 7 /.

By numerically computing the integral (1) in the two cases, one obtains

$$|\Delta s(t)| = 1.74\beta \frac{\rho_1}{\rho_0} r^*(t) \qquad (3')$$

$$|\Delta s(t)| = 2.41\beta \frac{\rho_1}{\rho_0} r^*(t) \qquad (3'')$$

For the cylindrical and spherical cases, respectively, the number of fringes N(t) corresponding to (3') and (3") evaluated from $|\Delta s(t)| = N(t).\ \lambda/2$

$$N(t) = 8.04 \frac{\rho_1}{\rho_0} \left[\frac{E_p}{\ell\ \rho_1}\right]^{\frac{1}{4}} t^{\frac{1}{4}} \qquad (4')$$

$$N(t) = 11.13 \frac{\rho_1}{\rho_0} \left(\frac{E_p}{\rho_1}\right)^{1/5} t^{2/5} \qquad (4'')$$

where ℓ is the plasma column length which was plotted using SFR photographic recordings and E_p represents the laser energy stored into the plasma source.

Good agreement was found between our experimental results and the theoretical predictions derived before (see Figure 3).

We notice that a "saddle point" was systematically recorded after (20 ÷ 30)μs from the interferogram origin, depending on the incident energy of the laser pulse. We supposed it to be due to a change in the sign of the optical path variation, appearing by the breaking of the shock wave border and the subsequent turbulent density change. Actually, one may estimate from the relation

$$p = \frac{2}{\gamma+1}\rho_1 c^2 \tag{5}$$

where $c = \frac{1}{2}\left(\frac{E_p}{\alpha\rho_1}\right)^{\frac{1}{4}} t^{\frac{1}{4}}$ and $c = \left(\frac{E_p}{\rho_1}\right)^{1/5} t^{-3/5}$ in the cylindrical and spherical cases respectively that the pressure on the shock wave border p, corresponding to these times, approaches the neighbouring gas pressure. For this reason we confined ourselves in examining the number of fringes registered till the saddle point moment.

Thus, by analysing the first part of a great number of interferograms we concluded that for small incident power densities, I, the experimental fringe number dependence on time is very close to the computed curve for the spherical case. For higher power densities, when a threshold value of $(2\div5)\times 10^7$ W/cm^2 (depending only on the irradiation conditions) is surpassed, the experimental points lie in the neighbourhood of the curves corresponding to the cylindrical case. At later times (typically after $(4\div6)\mu s$) in both cases the experimental points are placed in the proximity of the curve computed for the spherical case. One has to assume then that the shock waves propagating through the ambient atmosphere modify their initial expansion symmetry from spherical to cylindrical, when the incident power density initiating the plasma source exceeds a threshold value. Further on, both "spherical and cylindrical" shock waves approach a spherical expansion symmetry.

We correlated such a behaviour with the plasma source expansion symmetry. As it is known /1-4/, when I exceeds not only the breakdown threshold intensity, but equally another characteristic value (the laser threshold intensity of a laser supported detonation wave), the breakdown plasma detaches from the target and the ionization front propagates in a direction opposite to that of the laser beam. In this case, the plasma dimension along the laser beam is considerably larger than its transverse area and the plasma column acts as a source of a cylindrical blast wave. On the other hand, at lower incident intensities there is no detachment from the target and the plasma expands symmetrically into the surrounding gas. It follows then that the plasma may be looked upon as the source of a spherical blast wave.

From the beforementioned considerations one has to conclude that for the first stage of its existence, the shock wave propagating through the ambient gas takes over the plasma source expansion symmetry. At later times, generally subsequent to the laser pulse end, its expansion becomes spherical, regardless of the initial conditions.

REFERENCES

/1/ A.N.Pirri, R.Schlieer, D.Northam, Appl.Phys.Lett., 21, 79 (1972)

/2/ Yu.P.Raizer, J.E.T.P., 21, 1009 (1965)

/3/ A.I.Barchukov, F.B.Bunkin, V.I.Konov, A.M.Prokhorov, Letters to J.E.T.P., 17, 413 (1973)

/4/ I.Apostol, D.Drăgulinescu, C.Grigoriu, I.N.Mihăilescu, I.Morjan, Al.Niţoi, I.M.Popescu, M.Udrea, V.I.Konov, Proc. XIIth I.C.P.I.G. Eindhoven, 337 (1975)

/5/ W.E.Maher, R.B.Hall, J.Appl.Phys., 46, 761 (1975)

/6/ I.Apostol, D.Drăgulinescu, C.Grigoriu, I.N.Mihăilescu, Al.Nitoi, I.M.Popescu, Rev.Roum.Phys., 18, 1185 (1973)

/7/ L.I.Sedov, "Similarity and Dimensional Methods in Mechanics", Academic Press Inc., London (1959)

/8/ I.D.Apostol, E.Cojocaru, I.N.Mihăilescu, I.Morjan, V.A.Batanov, to be published in Rev.Roum.Phys. (1978)

FIGURE CAPTIONS

Figure 1 — Experimental arrangement and incident laser pulse shape on target: 1) double discharge TEA-CO_2, (2) KCl flats, (3) pyroelectric detector, (4) thermopile head, (5) BaF_2 lens, (6) plane metallic target, (7) plasma, (8) He-Ne laser, (9) silvered-glass beam-splitters, (10) silvered mirrors, (11) photo-detectors.

Figure 2 — Typical interferograms

Figure 3 — Fringe number dependence on time, N(t): experimental results and prediction based on the theory of intense explosions in gases for the cylindrical (5) and spherical (s) cases. The third curve (c+s) represents computations performed with the cylindrical approximation till $(4 \div 6)\mu s$ and with the spherical one from that point on.

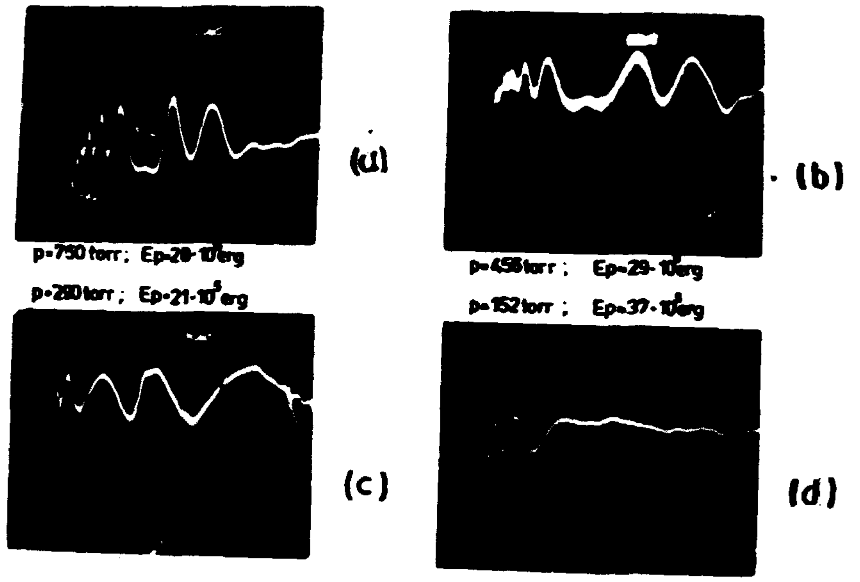
(a)
(b)
p=750 torr; Ep=28·10 erg
p=456 torr; Ep=29·10 erg
p=280 torr; Ep=21·10^5 erg
p=152 torr; Ep=37·10 erg
(c)
(d)

Fig. 2

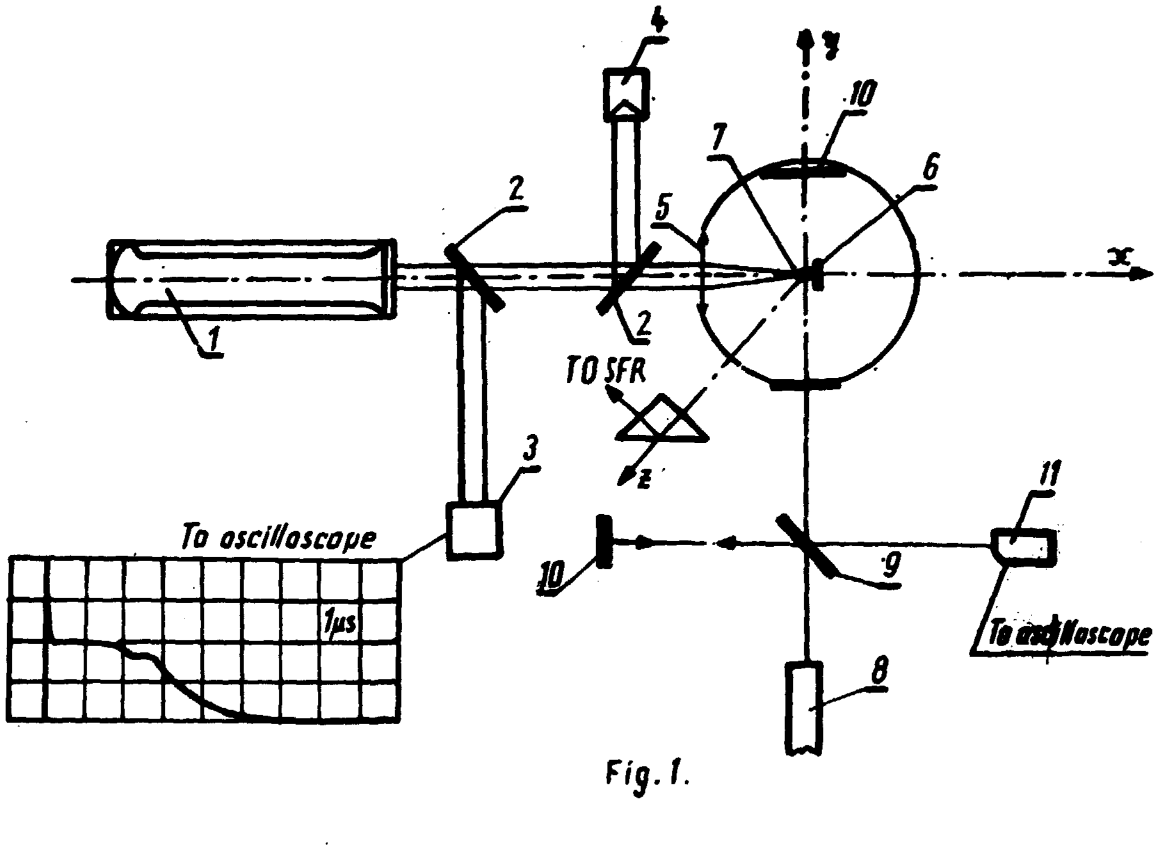
4
y
10
7
6
2
5
x
1
2
TO SFR
z
3
11
To oscilloscope
10
9
1μs
To oscilloscope
8

Fig. 1.

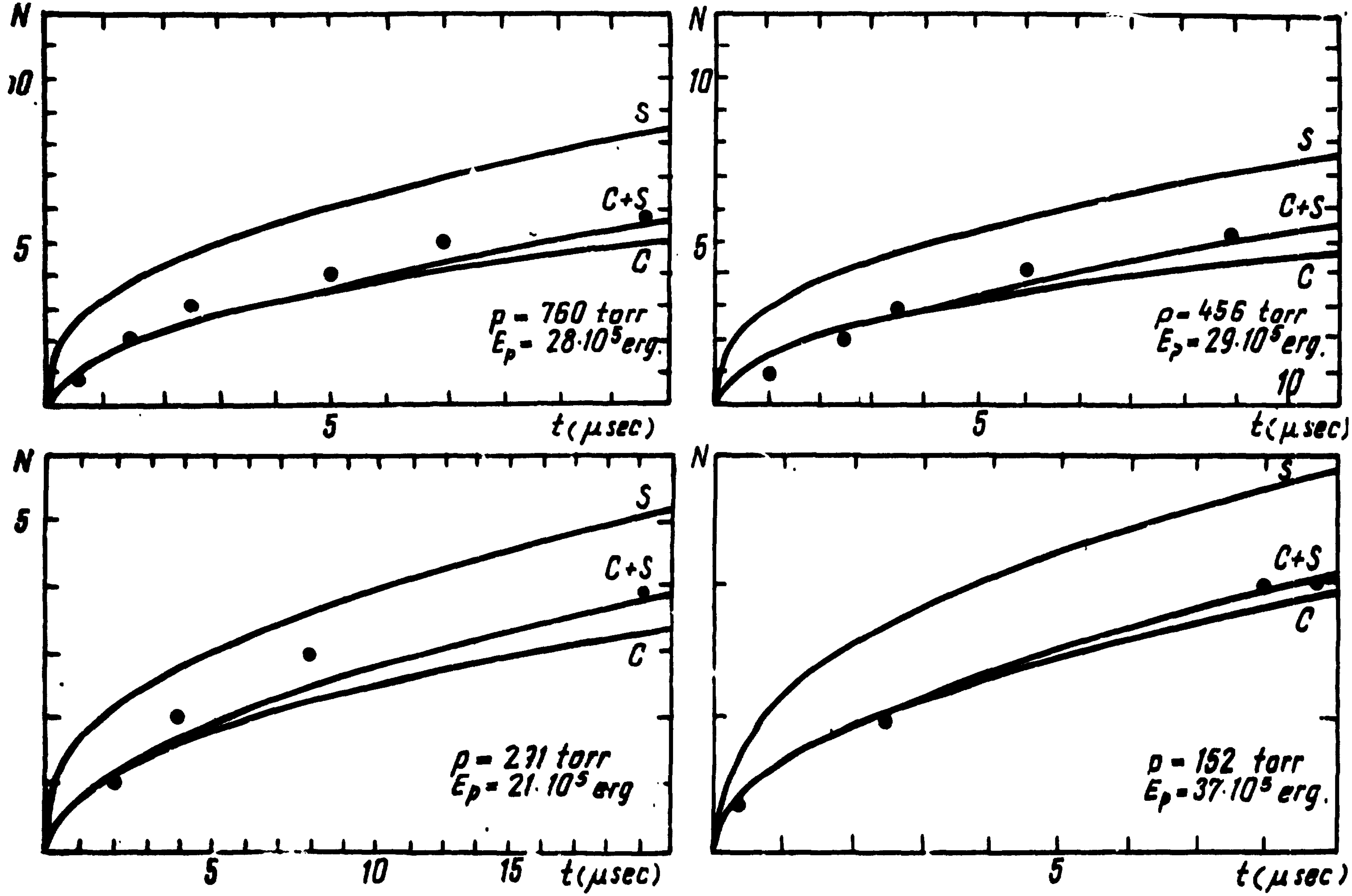
N
10
5
S
C+S
C
p = 760 torr
Ep = 28·10^5 erg.
5
t (μsec)
N
10
5
S
C+S
C
p = 456 torr
Ep = 29·10^5 erg.
10
5
t (μsec)
N
5
S
C+S
C
p = 231 torr
Ep = 21·10^5 erg
5
10
15
t (μsec)
N
S
C+S
C
p = 152 torr
Ep = 37·10^5 erg.
5
t (μsec)

Fig.3